A Numerical Study on Heat Transfer Characteristics in a Spray Column Direct Contact Heat Exchanger

Yong Heack Kang
Korea Institute of Energy Research, Taejeon 305-343, Korea
Nam Jin Kim
Graduate School, Inha University, Inchon 402-751, Korea
Byung Ki Hur
Department of Biological Engineering, Inha University, Inchon 402-751, Korea
Chong Bo Kim*
Department of Mechanical Engineering, Inha University, Inchon 402-751, Korea

A reliable computational heat transfer model has been investigated to define the heat transfer characteristics of a spray column direct contact heat exchanger, which is often utilized in the process involving counterflows for heat and mass transfer operations. Most of the previous studies investigated are one-dimensional unsteady solutions based on rather fragmentary experimental data. Development of a multidimensional numerical model and a computational algorithm are essential to analyze the inherent multidimensional characteristics of a direct contact heat exchanger. The present study has been carried out numerically and establishes a solid simulation algorithm for the operation of a direct contact heat exchanger. Operational and system parameters such as the speed and direction of working fluid droplets at the injection point, and the effects of aspect ratio and void fraction of continuous fluid are examined thoroughly as well to assess their influence on the performance of a spray column.

Key Words : Direct Contact, Spray Column, Heat Exchanger, Continuous Fluid, Dispersed Fluid

Nomenclature

b : Height of lateral inlet opening (m)
C_D : Drag force coefficient
D : Diameter of spray column (m)
d : Diameter of dispersion plate (m)
F_r : Interfacial resistance coefficient (kg/sec)
g : Acceleration due to gravity (9.81 m/sec^2)
H : Enthalpy (kJ/kg)
K : Thermal conductivity (kJ/m · sec · ℃)
L : Length of spray column (m)
l : Length of inlet piping (m)
Nd : Number of droplet
Nu : Nusselt number
P : Pressure (N/m^2)
Pr : Prandtl number
R : Droplet radius (m)
Re : Reynolds number
T : Temperature (℃)
Uv : Volumetric heat transfer coefficient (W/m^3 · ℃)
V : Velocity (m/sec)
α : Thermal diffusivity (m^2/sec)
ε : Volume fractions of continuous fluid
μ : Viscosity (kg/m · sec)
ρ : Density (kg/m^3)
ϕ : Volume fraction of dispersed fluid

Subscript

c : Continuous fluid
d : Dispersed fluid
r : Radial coordinate
x : Axial coordinate

* Corresponding Author,
E-mail : cbkim@inha.ac.kr
TEL : +82-32-860-7313; **FAX** : +82-32-868-1716
Department of Mechanical Engineering, Inha University, Inchon 402-751, Korea. (Manuscript **Received** August 9, 2000; **Revised** January 2, 2002)

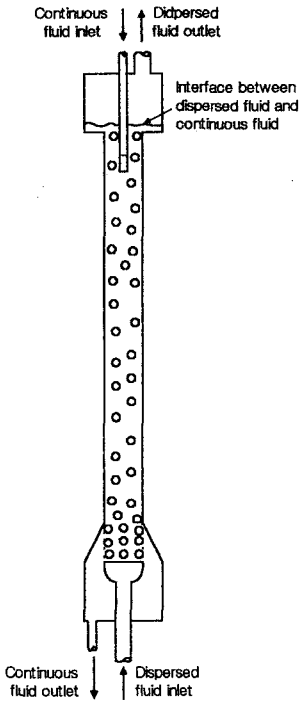

Fig. 1 Spray column direct contact heat exchanger

1. Introduction

Direct contact heat exchangers offer a highly efficient means of transferring heat between two immiscible fluids(Wright, 1988). They presently are used in chemical engineering, geothermal utilization and manufacturing(Boehm and Kreith, 1988). As shown in Fig. 1, the fundamental operating principle of direct contact heat exchangers is to bring two fluids in direct contact with each other within a cylindrical tube or column. The fluids pass in either a concurrent or counterflow direction with the latter being the more common.

Heat exchange between the continuous and dispersed fluids occurs by convection between the stream of droplets travelling through the continuously moving medium. Since the natural buoyancy of the two liquids creates a rise and fall mechanism, an adequate density differential must exist. This differential can perhaps be counted among the limitations of these systems albeit not too strictly restrictive one given the wide range of possible fluid candidates(Brickman and Boehm, 1995). Direct contact heat exchangers have many merits such as 1) high efficiency due to the possibly close temperature approaches, 2) no fouling, 3) reduced capital costs due to elimination of the metallic tubing interface to name a few(Kim, 1987).

Many creditable studies about the merits of heat exchanger have been done. Yang and Yeh (1966) studied numerically the growth and formation of a single droplet. Coban and Beohm (1986) calculated the temperature of a continuous fluid with a one-dimensional steady state flow model. Stamps et al. (1986) developed a heat transfer model for a liquid-liquid spray column employing a one-dimensional dispersion model. Kim and Jacobs(1986) investigated numerically spray column direct contact heat exchangers by using a continuous phase two-dimensional axisymmetric flow model. The results have shown that an axial injection produced a strong jet concentrated on the center line of the column, while a radial release of the continuous phase provided a near uniform flow in the column.

Jacobs and Golafshani(1989) investigated a model using the assumption of no drop internal resistance to heat transfer and another where the heat transfer was governed by diffusion within the drop. The latter model showed the better agreement with the temperature profile data, expecially when it accounted for the drop growth. Kang and Kim(1994) analyzed a spray column direct contact heat exchanger with a two- dimensional axisymmetric two-component flow model. They showed that radial injection for the continuous flow was advantageous in obtaining desirable uniform velocity distributions. As the aspect ratio increased and the inlet velocity decreased, flow patterns in a spray column were shown to have a better uniform velocity distribution.

Brickman and Boehm(1995) developed a one-dimensional modelling for a spray column type direct contact heat exchanger with a sieve tray enhancement. Song et al. (1998) showed an approximately proportional relationship between the evaporation height and the reciprocal of the driving temperature difference.

In order to define the heat transfer characteristics in a spray column direct contact

heat exchanger, development of a multidimensional numerical model and a computational algorithm is essential. It is also necessary to analyze the inherent multidimensional characteristics of a direct contact heat exchanger. So the present study has been carried out numerically based on the two-dimensional axisymmetric two-component flow model of Kang and Kim(1994) for the operation of a direct contact heat exchanger. Operational and system parameters such as the injection velocity, void fraction, aspect ratio and injection temperature of each fluid are examined thoroughly to assess their influence on the performance of spray column type direct contact heat exchangers.

2. Mathematical Modeling

2.1 Governing equation

2.1.1 Continuity equation

The continuity equations for the continuous and the dispersed fluids are,

$$\frac{\partial}{\partial x}(\varepsilon\rho_c V_{cx})+\frac{1}{r}\frac{\partial}{\partial r}(\varepsilon r\rho_c V_{cr})=0 \quad (1)$$

and

$$\frac{\partial}{\partial x}(\phi\rho_d V_{dx})+\frac{1}{r}\frac{\partial}{\partial r}(\phi r\rho_d V_{dr})=0 \quad (2)$$

where ε and ϕ are the volume fractions of continuous and dispersed fluid, respectively.

2.1.2 Momentum equation

For the continuous fluid, the momentum equations along the axial and the radial directions are, respectively,

$$\frac{\partial}{\partial x}(\varepsilon\rho_c V^2_{cx})+\frac{\partial}{\partial r}(\varepsilon\rho_c V_{cr}V_{cx}) = -\varepsilon\frac{\partial P}{\partial x}+\varepsilon\mu_c\left(\frac{\partial^2 V_{cx}}{\partial r^2}+\frac{1}{r}\frac{\partial V_{cx}}{\partial r}+\frac{\partial^2 V_{cx}}{\partial x^2}\right) -\varepsilon F_x(V_{cx}-V_{dx}) \quad (3)$$

and

$$\frac{\partial}{\partial x}(\varepsilon\rho_c V_{cx}V_{cr})+\frac{\partial}{\partial r}(\varepsilon\rho_c V^2_{cr}) = -\varepsilon\frac{\partial P}{\partial r}+\varepsilon\mu_c\left(\frac{\partial^2 V_{cr}}{\partial r^2}+\frac{1}{r}\frac{\partial V_{cr}}{\partial r}+\frac{\partial^2 V_{cr}}{\partial x^2}-\frac{V_{cr}}{r^2}\right)-\varepsilon F_r(V_{cr}-V_{dr}) \quad (4)$$

For the dispersed fluid, the momentum equation along the axial direction s,

$$\frac{\partial}{\partial x}(\phi\rho_d V^2_{dx})+\frac{\partial}{\partial r}(\phi\rho_d V_{dr}V_{dx}) = -\phi\frac{\partial P}{\partial x}+\phi\mu_d\left(\frac{\partial^2 V_{dx}}{\partial r^2}+\frac{1}{r}\frac{\partial V_{dx}}{\partial r}+\frac{\partial^2 V_{dx}}{\partial x^2}\right) -\phi F_x(V_{dx}-V_{cx})+\phi g(\rho_c-\rho_d) \quad (5)$$

and, along the radial direction,

$$\frac{\partial}{\partial x}(\phi\rho_d V_{dx}V_{dr})+\frac{\partial}{\partial r}(\phi\rho_d V^2_{dr}) = -\phi\frac{\partial P}{\partial r}+\phi\mu_d\left(\frac{\partial^2 V_{dr}}{\partial r^2}+\frac{1}{r}\frac{\partial V_{dr}}{\partial r}+\frac{\partial^2 V_{dr}}{\partial x^2} -\frac{V_{dr}}{r^2}\right)-\phi F_r(V_{dr}-V_{cr}) \quad (6)$$

where friction factor F_r is given by,

$$Fr=-\frac{3}{8}\frac{\phi}{R_d}C_D\rho_c|V_d-V_c|(V_c-V_d) \quad (7)$$

For the mixture, the total momentum equation is obtained by adding the equations of each fluid. Therefore, the equations on the axial and the radial directions can be described as, respectively,

$$\frac{\partial}{\partial x}(\varepsilon\rho_c V^2_{cx})+\frac{\partial}{\partial r}(\varepsilon\rho_c V_{cr}V_{cx})+\frac{\partial}{\partial x}(\phi\rho_d V^2_{dx}) +\frac{\partial}{\partial r}(\phi\rho_d V_{dr}V_{dx})=-\varepsilon\frac{\partial P}{\partial x}-\phi\frac{\partial P}{\partial x} +\varepsilon\mu_c\left(\frac{\partial^2 V_{cx}}{\partial r^2}+\frac{1}{r}\frac{\partial V_{cx}}{\partial r}+\frac{\partial^2 V_{cx}}{\partial x^2}\right)+\phi\mu_d \left(\frac{\partial^2 V_{dx}}{\partial r^2}+\frac{1}{r}\frac{\partial V_{dx}}{\partial r}+\frac{\partial^2 V_{dx}}{\partial x^2}\right)+\phi g(\rho_c-\rho_d) \quad (8)$$

and,

$$\frac{\partial}{\partial x}(\varepsilon\rho_c V_{cx}V_{cr})+\frac{\partial}{\partial r}(\varepsilon\rho_c V^2_{cr})+\frac{\partial}{\partial x}(\phi\rho_d V_{dx}V_{dr}) +\frac{\partial}{\partial r}(\phi\rho_d V^2_{dr})=-\varepsilon\frac{\partial P}{\partial r}-\phi\frac{\partial P}{\partial r}+\varepsilon\mu_c\left(\frac{\partial^2 V_{cr}}{\partial r^2} +\frac{1}{r}\frac{\partial V_{cr}}{\partial r}+\frac{\partial^2 V_{cr}}{\partial x^2}-\frac{V_{cr}}{r^2}\right)+\phi\mu_d\left(\frac{\partial^2 V_{dr}}{\partial r^2} +\frac{1}{r}\frac{\partial V_{dr}}{\partial r}+\frac{\partial^2 V_{dr}}{\partial x^2}-\frac{V_{dr}}{r^2}\right) \quad (9)$$

2.1.3 Energy equation

The energy equation for the continuous fluid can be described as,

$$\frac{\partial}{\partial x}(\varepsilon c_c\rho_c V_{cx}T_c)+\frac{\partial}{\partial r}(\varepsilon c_c\rho_c V_{cr}T_c)$$

$$=-U_v(T_c-T_d) \tag{10}$$

and for the dispersed fluid,

$$\frac{\partial}{\partial x}(\phi\, c_d\rho_d V_{dx}T_d)+\frac{\partial}{\partial r}(\phi\, c_c\rho_d V_{dr}T_d) =-U_v(T_d-T_c) \tag{11}$$

For the mixture, the total energy equation is obtained by adding the equations of each fluid,

$$\frac{\partial}{\partial x}(\varepsilon\rho_c V_{cx}H_c)+\frac{\partial}{\partial x}(\phi\,\rho_d V_{dx}H_d) +\frac{\partial}{\partial r}(\varepsilon\rho_c V_{cr}H_c)+\frac{\partial}{\partial r}(\phi\,\rho_d V_{dr}H_d)=0 \tag{12}$$

The volme fraction relation on the continuous and the dispersed fluids in a spray column is as follow,

$$\varepsilon+\phi=1 \tag{13}$$

2.2 Heat transfer modelling

If the heat transfer of a droplet of the continuous fluid is governed both by the inner conduction and the outer convection, the heat transfer per a specific volume is described as the following equation,

$$\begin{aligned} Q/Vol &= U_v\Delta T \\ &= K_d(N_d 4\pi R_d^2)\frac{\partial T_d}{\partial r}\Big|_{r=R_d} \\ &= \frac{3}{2}\frac{\phi}{R_d^2}h_0(T_{d(r=R_d)}-T_c) \end{aligned} \tag{14}$$

where K_d is the inner heat transfer coefficient of droplet, N_d is the numbers of droplets and R_d is the radius of droplet. Surface temperature $T_{d(r=R_d)}$ is obtained by solving Eq. (15),

$$\frac{\partial T_d}{\partial t_1}=\frac{\alpha_d}{r^2}\frac{\partial}{\partial r}\left(r^2\frac{\partial T_d}{\partial r}\right) \tag{15}$$

where t_1 is defined as the time measured from the instance a droplet begins to rise through the column, and the associated initial and the boundary conditions are,

$$\begin{aligned} &T_d=T_{do}(t_1=0) \\ &T_d=finite(r=0) \\ &K_d\frac{\partial T_d}{\partial r}\Big|_{r=R_d}=h_o(T_{d(r=R_d)}-T_c) \end{aligned} \tag{16}$$

where h_o is the outer heat transfer coefficient of a droplet. Jacobs(1991) recommends the following correlation for h_o,

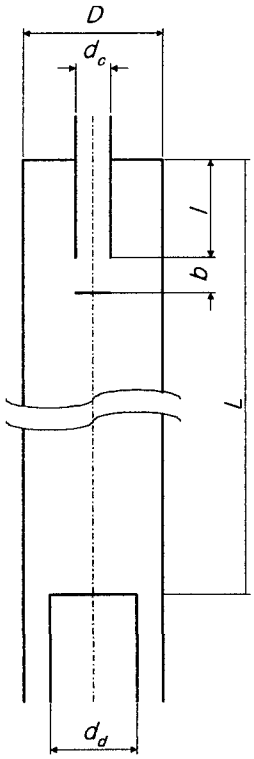

Fig. 2 Calculation domain

$$Nu_D=3.1Re_d^{0.37}Pr_c^{1/3} \tag{17}$$

3. Numerical Methods

The calculation domain of this study is shown in Fig. 2. The follwing dimensions are fixed; D=1m, d_c=0.1667m, d_d=0.6667m, l=1m and b=0.4m. Brine and isobutane are used as the continuous and the dispersed fluids, respectively. The numerical solutions are performed with the aspect ratio(L/D), 3, 5, 7 and 10, the injection velocity of the continuous fluid, 0.1, 0.25, 0.50 and 0.75m/sec, and that of the dispersed fluid, 0.016, 0.030, 0.08 and 0.130m/sec. The heat transfer characteristics of the mixed fluid are examined with the inlet temperatures of the dispersed fluid of 40℃ and 60℃, while those of the continuous fluid, 60℃ and 80℃, the void fractions, 0.05, 0.1 and 0.2.

In order to solve the governing equations, the SIMPLEC algorithm with the hybrid scheme in a staggered grid of 27×14 is used with an axisy-

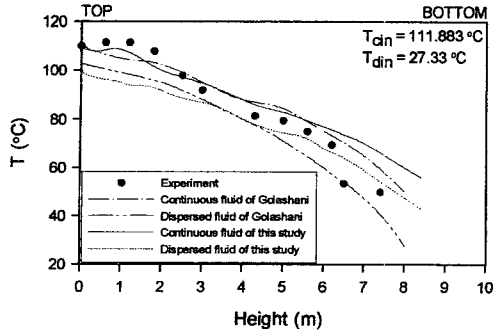

Fig. 3 Temperature profiles of continuous(Tc) and dispersed fluid(Td) along the column at $\dot{m}_c$=11.698kg/sec and $\dot{m}_d$=12.259kg/sec

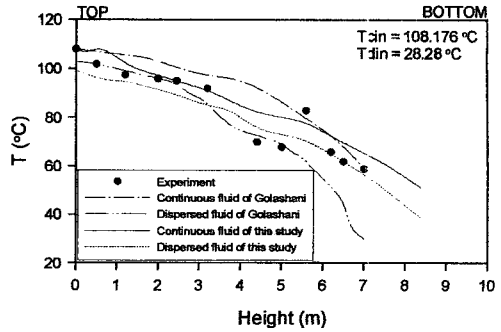

Fig. 4 Temperature profiles of continuous(Tc) and dispersed fluid(Td) along the column at $\dot{m}_c$=7.623kg/sec and $\dot{m}_d$=7.379kg/sec

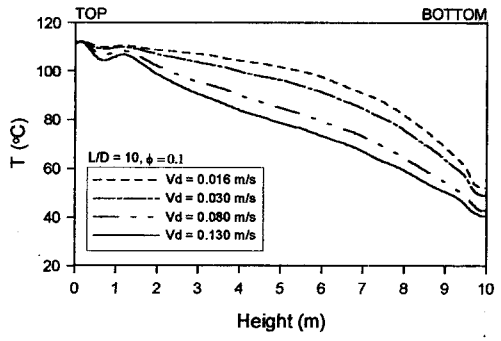

Fig. 5 Temperature profiles of continuous fluid(Tc) along the column at the various dispersed fluid velocity(Vd) and Vc=0.5m/sec

mmetric irregular interval along the x-direction and a regular interval along the r-direction. Also when the residual mass imbalance becomes 4.0× 10E-3 or less, the calculation is terminated.

Because of the recirculation, the irregular interval grid along the x-direction is densely made around the injection nozzle, and the grid interval at the center is larger than that around the nozzle. The numerical calculation is performed along the proceeding direction of the dispersed fluid, and the value of the constant and the droplet diameter of the dispersed fluid as proved reliable in the range over the Reynolds number 104 by Jacobs and Golafshani(1989) are used. Also in order to reduce the error for the calculation of the mean temperature of the dispersed fluid, Romberg integral(Jacobs and Golafshani, 1989) is used.

4. Results and Discussions

4.1 Comparisons between the experimental and the numerical results

Figures 3 and 4 present the temperature measured throughout the 500kW spray column (Olander et al. , 1983) and the one-dimensional result of Jacob and Golafshani (1989) and the result of this study using a two-dimensional flow model. The model of this study predicts more exactly the physical phenomena in a spray column than that of the one-dimensional flow model. The error between the experimental and the numerical data are under 8% at the upper part and under 20% at the lower part of the column in case of high fluid velocity (Fig. 3). However, at the low velocity, the error is only 10% at the bottom of the spray column.

4.2 Fluid temperature according to the injection velocity

The temperature profiles of each fluid along the column height at the injection velocity of the continuous fluid of 0.5m/s and that of the dispersed fluid of 0.016, 0.030, 0.080 and 0.13 m/s are shown in Figs. 5 and 6. Figures 7 and 8 show the temperature profiles at the injection velocity of the dispersed fluid of 0.08m/s and that of the continuous fluid of 0.10, 0.25, 0.50 and 0. 75m/s. In Figs. 4 and 5, as the injection velocity of dispersed fluid increases, the temperatures of two fluids decrease and the decreasing rate is slower. Because the local back mixing around the injection nozzle occurs strongly as the injection

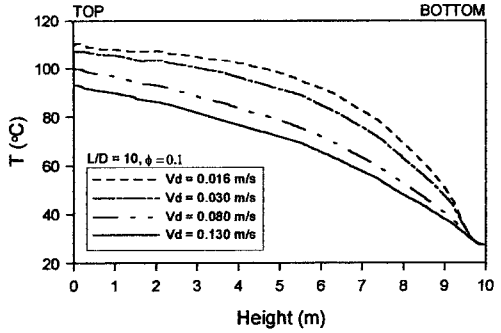

Fig. 6 Temperature profiles of dispersed fluid(Td) along the column at the various dispersed fluid velocity(Vd) and Vc=0.5m/sec

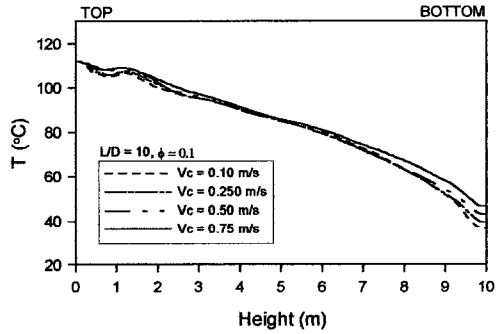

Fig. 7 Temperature profiles of continuous fluid(Tc) along the column at the various continuous fluid velocity(Vc) and Vd=0.08m/sec

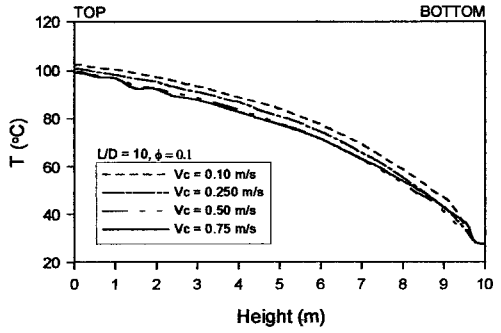

Fig. 8 Temperature profiles of dispersed fluid(Td) along the column at the various continuous fluid velocity(Vc) and Vd=0.08m/sec

velocity of the dispersed fluid increases, the fluid temperature changes in a wavy manner at the upper part of the column.

In Figs. 7 and 8, as the injection velocity of the dispersed fluid increases, the temperature change

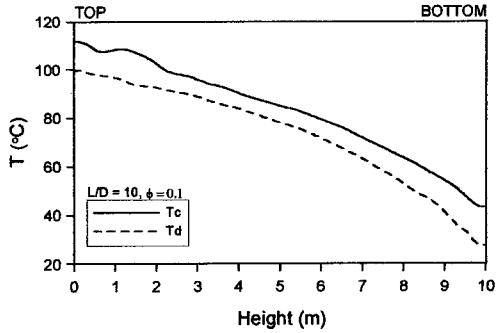

Fig. 9 Temperature profiles of continuous(Tc) and dispersed fluid(Td) along the column at Vc=0.5m/sec and Vd=0.08m/sec

rates of the two fluids are much lower than those of the previous results. As the injection velocity of the continuous fluid increases, the temperature of the dispersed fluid decreases, but the temperature of the continuous fluid increases at the upper part of the column. Therefore, the injection velocity of the dispersed fluid is a key parameter among the working conditions.

4.3 Fluid temperature according to the aspect ratio(L/D)

The temperature profiles of two fluids at the various aspect ratios(10, 7, 5, and 3) are shown in Fig. 9 to 12 for the injection velocities of 0.5m/s for the continuous fluid and 0.08m/s for the injection velocity where void fraction is being 0.1. The results show that where the aspect ratio is relatively small, the temperatures of the two fluids change rather rapidly and the temperature difference of the two fluids becomes large between the inlet and the outlet of the column. These results indicate that the formation of uniform flow within the column has an advantage to improve heat transfer rates especially at smaller aspect ratios, where the temperature difference between the outlet temperature of the dispersed fluid and that of the continuous fluid is small.

When the aspect ratio of the column is small, the temperature of the continuous fluid is strongly affected by the back flow mixing within the column. The results show that the formation of the back flow is strongly related to column height,

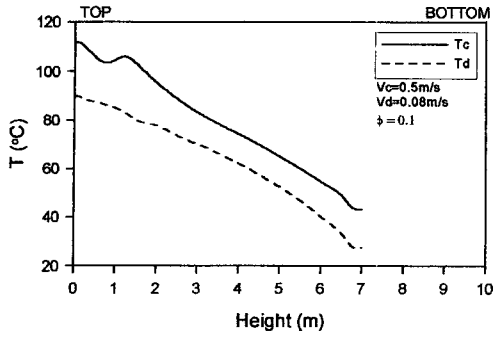

Fig. 10 Temperature profiles of continuous(Tc) and dispersed fluid(Td) along the column of L/D=7

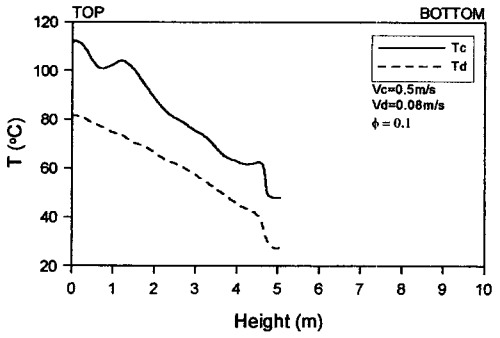

Fig. 11 Temperature profiles of continuous(Tc) and dispersed fluid(Td) along the column of L/D=5

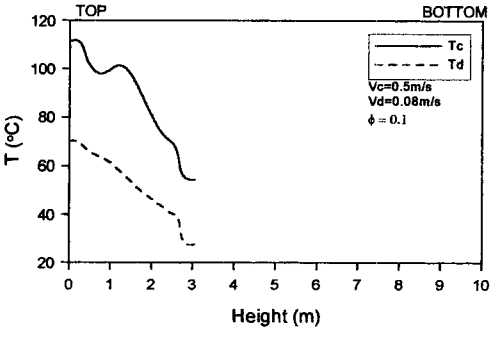

Fig. 12 Temperature profiles of continuous(Tc) and dispersed fluid(Td) along the column of L/D=3

and consequently the heat transfer rates become to give higher values by these flow behavior.

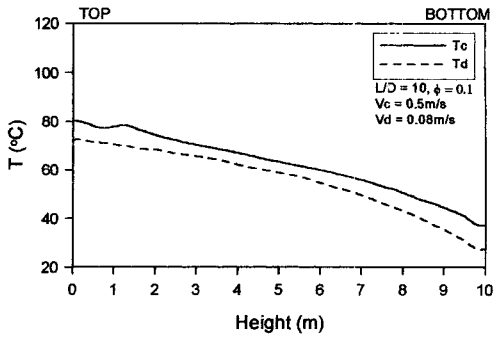

Fig. 13 Temperature profiles of continuous(Tc) and dispersed fluid(Td) along at Tcin=80℃ and Tdin=27.33℃

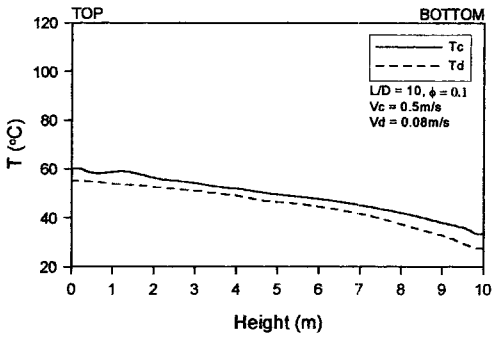

Fig. 14 Temperature profiles of continuous(Tc) and dispersed fluid(Td) along the column at Tcin=60℃ and Tdin=27.33℃

4.4 Fluid temperature according to the injection temperature

Figures 13 and 14 show the change of the two fluid temperatures according to the injection temperature variation of the continuous fluid of 60℃ and 80℃ with the dispersed fluid at 27.33℃, the aspect ratio of 10 and the injection velocities of the continuous and the dispersed fluids of 0.5m/s and 0.08m/s, respectively. The temperature change of the two fluids according to the injection temperature variation of the dispersed fluid of 40℃ and 60℃ and that of the continuous fluid of 11.88℃ are shown in Figs. 15 and 16. As the injection temperature of the dispersed fluid is fixed and that of the continuous fluid is low, the temperature difference between the two fluids becomes small along the height.

As the injection temperature of the continuous fluid is fixed and that of the dispersed fluid is low,

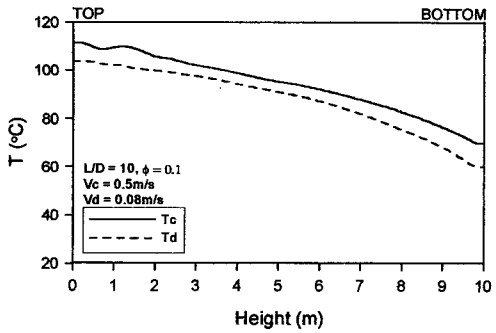

Fig. 15 Temperature profiles of continuous(Tc) and dispersed fluid(Td) along the column at Tcin=111.88℃ and Tdin=60℃

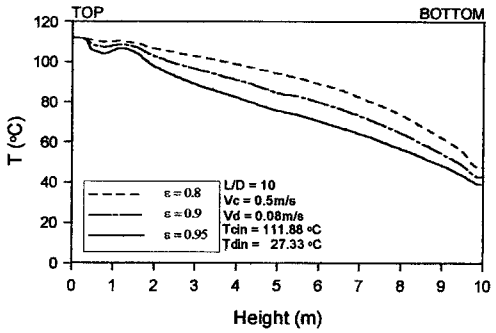

Fig. 17 Temperature profiles of continuous fluid (Tc) along the column at the various void fraction of continuous fluid(ε)

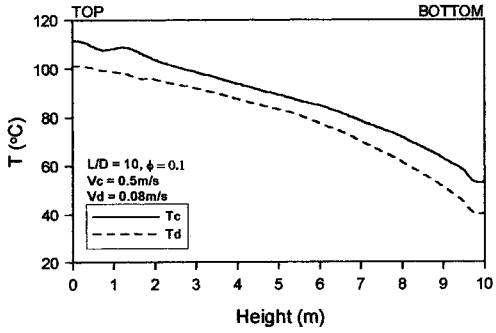

Fig. 16 Temperature profiles of continuous(Tc) and dispersed fluid(Td) along the column at Tcin=111.88℃ and Tdin=40

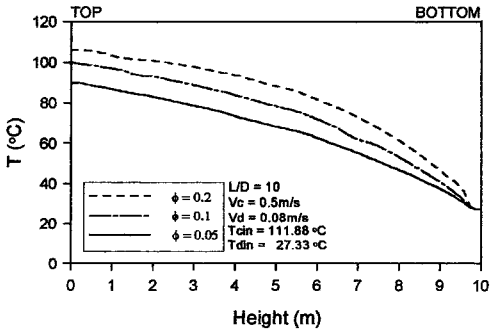

Fig. 18 Temperature profiles of dispersed fluid(Td) along the column at the various void fraction of dispersed fluid(ϕ)

the temperature difference between two fluids becomes small. Therefore, the lower the initial temperature difference between the fluids is, the smaller is the difference of the two temperatures along the height. This means that a spray column direct contact heat exchanger can be effectively applied to solar energy systems and waste heat recovery systems, etc.

4.5 Fluid temperature according to the void fraction

Figures 17 and 18 show the temperature change of each fluids according to the variation of the void fraction at the injection velocity of the continuous fluid of 0.5 m/sec and that of the dispersed fluid of 0.08m/sec.

As the void fraction of the continuous fluid decreases, the temperature becomes low along the height and the decreasing rate becomes high in the middle of the column. As the void fraction increases, the temperature difference between the two fluids becomes high along the height. Since the void fraction is not a parameter which can be changed in the middle of operation, an optimal void fraction must be selected in advance according to the dispersed fluid and the application purpose.

4.6 Characteristics of volume heat transfer coefficient

The changes of the volume heat transfer coefficient(U_v) according to the change of flow rates of each fluid are shown in Figs. 19 to 21. The local volume heat transfer coefficient along the height is almost uniform to the middle of the column, but it is later highly affected by the back mixing from the top of the column to the inlet nozzle of the continuous fluid.

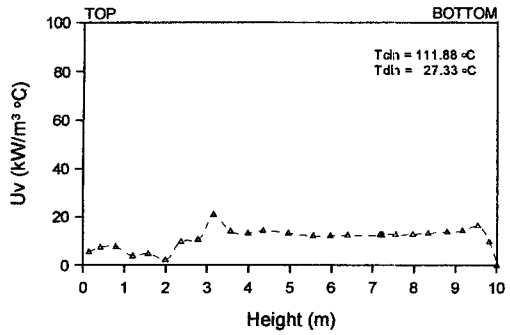

Fig. 19 Volumetric heat transfer coefficient variation along the column at $\dot{m}_c$=7.623kg/sec and $\dot{m}_d$=3.173kg/sec

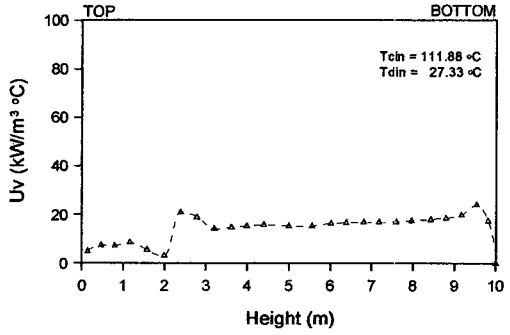

Fig. 20 Volumetric heat transfer coefficient variation along the column at $\dot{m}_c$=11.443kg/sec and $\dot{m}_d$=7.379kg/sec

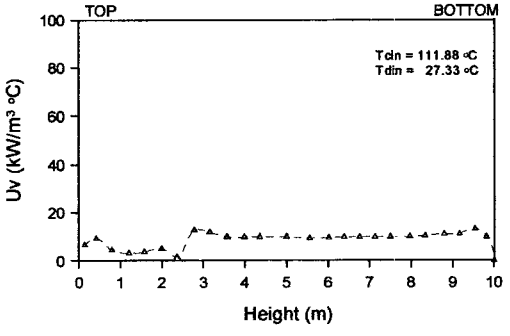

Fig. 21 Volumetric heat transfer coefficient variation along the column at $\dot{m}_c$=11.443kg/sec and $\dot{m}_d$=3.173kg/sec

As the flow rate of the dispersed fluid increases, the volume heat transfer coefficient increases along the height, but the trend is reversed for the case of the continuous fluid. When the flow rates of each fluid change, the local volume heat transfer coefficient also changes around the injection nozzle of the continuous fluid because of the different mixing pattern of each fluid. The figures show that as the flow rates of the two fluids increase, the local increase in the heat tramsfer coefficient occurs near the injection nozzle of the continuous fluid.

5. Conclusions

The computational results on the heat transfer characteristics in a spray column direct contact heat exchanger using a two-dimensional axisymmetric two-component flow model are summarized as follows :

(1) The proposed multi-dimensional flow model predicts the physical phenomena more closely in a spray column than the previous one -dimensional flow model.

(2) The injection velocity of the dispersed fluid is a key parameter among the working conditions.

(3) The formation of the bank flow relates to the change of the column height, while the heat transfer is significantly influenced by the change in the flow rates.

(4) The lower the initial temperature difference between the fluids is, the closer is the difference along the height.

(5) The local volume heat transfer coefficient along the height is almost uniform up to the middle of the column, however, it is significantly affected by back mixing at the top of the column where the inlet of the continuous fluid is located.

References

Boehm, R. F. and Kreith, F., 1988, *Direct Contact Heat Transfer Process, Direct Contact Heat Transfer*, Hemisphere Publishing Co., pp. 1 ~24.

Brickman, R. A. and Boehm R. F., 1995, "Numerical Simulation and Comments on Sieve Tray Spray-Column Direct Contact Heat Exchangers," *Proceedings of the ASME Heat Transfer Division*, HTD-Vo. 317-1, pp. 459~467.

Coban, T. and Beohm, R., 1986, "Numerical and Experimental Modelling of Three Phase Di-

rect Contact Heat Exchangers," *Proceeding of the 8th Int. Heat Transfer Conference*, Vol. 6, pp. 3019~3024.

Jacobs, H. R., 1991, "Computational Model -ling of Multiphase Flows with One Phase Dispersed," US - JAPAN Joint Seminar, Tokyo.

Jacobs, H. R. and Golafshani, M., 1989, "Stability of a direct-contact spray column heat exchanger," *J. of Heat Transfer*, Vol. 111, pp. 767~772.

Jacobs, H. R. and Golafshani, M., 1989, "A Heuristic Evaluation of the Governing Mode of Heat Transfer in a Liquid-Liquid Spray Column," *J. of Heat Transfer*, Vol. 111, pp. 773~779.

Kim, S. H. 1987, "The Characteristics and Applications of High Performance Direct Contact Exchangers," *Magazine of SAREK*, Vol. 15, No. 2, pp. 109~115.

Kim, C. B. and Jacobs, H. R., 1987, "Numerical Study on the Operational Performance of Spray Column Direct Contact Heat Transfer," *KSME Journal*, Vol. 1, No. 1, pp. 9~12.

Kang, Y. H. and Kim, C. B., 1994, "A Numerical Analysis on Characteristics of the Flow in a Spray Column Direct Contact Heat Exchanger," *Solar Energy*, Vol. 14, No. 1, pp. 103~113.

Olander, R., Oshmyansku, S. Nichols, K., and Werner, D., 1983, "Final Phase Testing and Evaluation of the 500kWe Direct Contact Heat Exchange Pilot Plant at East Mesa," ERDA Report/DOE/SF/11700 T1, Arcada, CO.

Stamps, D. W., Barr, D. and Valenzuela, J. A., 1986, "A Model of the Heat Transfer in a Liquid -Liquid Spray Column," *J. of Heat Transfer, Trans. ASME*, Vol. 108, pp. 488~489.

Song, M., Steiff, A. and Weinspach, P. M., 1998, "Parametric Analysis of Direct Contact Evaporation Process in a Bubble Column," *Int. J. Heat Mass Transfer*. Vol. 41, No. 12, pp. 1749~1758.

Wright, J. D., 1988, *Design of Direct Contact Preheater/Boilers for Solar Pond Power Plants, Direct Contact Heat Transfer*, Hemisphere Publishing Co., pp. 299~334.

Yang, W. J. and Yeh, H. C., 1966, "Theoretical Study of Bubble Dynamics in Purely Viscous Fluids," *A. I. Ch. E. Journal*, Vol. 12, No. 5, pp. 927~931.